Pergamon

Int. J. Heat Mass Transfer. Vol. 41, No. 17, pp. 2581–2587, 1998

Printed in Great Britain
0017–9310/98 $19.00 + 0.00

PII: S0017–9310(97)00346–3

Radiative heat transfer in soot-containing combustion systems with aggregation

T. L. FARIAS and M. G. CARVALHO
Department of Mechanical Engineering, Institute Superior Técnico, 1096 Lisbon, Portugal

and

Ü. Ö. KÖYLÜ†
Department of Mechanical Engineering, Florida International University, Miami, FL 33174, U.S.A.

(*Received* 23 *January* 1997 *and in final form* 3 *November* 1997)

Abstract—The effects of soot shape on radiative transfer predictions in soot-containing flames were quantitatively analyzed by using a realistic simulation of the aggregation process. Various spectral properties (phase function, albedo, extinction coefficient, and emissivity) of fractal soot aggregates were computed using the integral equation formulation for scattering (IEFS) for a broad wavelength spectrum from ultraviolet (0.2 μm) to infrared (6.2 μm). Total emissions from uniform clouds of aggregates of small spherical particles were then estimated for typical soot volume fractions and flame temperatures. All spectral and total radiative transfer properties computed using IEFS were normalized by the predictions based on the primary (unaggregated) particles. The spectral variation of the extinction coefficient of aggregates relative to that of primary particles has a somewhat unexpected and complex behavior in the ultraviolet and infrared wavelength regions due to the opposite effects of morphology and soot refractive indices. The effects of soot aggregation on spectral and total emissivities are found to be less than 25 and 13%, respectively, for typical particle volume fractions and flame temperatures. The results suggest that the shape effects on emission predictions in soot-laden flames can be neglected, vastly simplifying the engineering treatment of radiation modeling of combustion devices.

1. INTRODUCTION

Radiative energy transfer in absorbing, emitting, and scattering media at high temperatures is of particular interest to those involved in many engineering technologies, including internal combustion engines, gas turbines, industrial furnaces, fire safety, and atmospheric radiation [1, 2]. It is well known that the presence of soot in most practical combustion systems enhances heat transfer rates significantly due to the continuum radiation in the visible and infrared regions of the wavelength spectrum. In addition to soot concentration and temperature distributions in such particulate-laden media, radiation predictions require information about the spectral radiative properties of soot, such as phase function, albedo, and emissivity, which are characterized in terms of the refractive index and size/morphology [3].

Early literature on soot radiation analysis in flames generally considered soot shape as spherical, so that simple predictions based on the Mie theory with a volume-equivalent diameter were possible. Unfortunately, ultra fine particles (including soot) produced in combustion systems form aggregates with a wide range of sizes and shapes [4, 5]. As a result of this complex morphology, the overall shape of aggregates was initially modeled as spheres, cylinders, prolate spheroids, etc. [6]. Because this permitted an analytical assessment of morphology effects on radiative properties of soot, several investigators also further explored similar limiting shapes [7, 8]. Such models obviously did not provide a quantitative description of soot radiation in flames. Consequently, Charalampopoulos and Chang [9], and Ku and Shim [10] investigated the effect of soot morphology on flame radiation by considering aggregates of small primary particles. Reference [9] demonstrated that the effect of shape on soot radiation for small aggregates of chain-like morphologies was relatively unimportant. Both of these studies, however, considered unrealistic chain-like small aggregates (less than 32 particles in an aggregate), which may not properly represent fractal-like soot morphologies [11]. Radiative properties of fractal soot aggregates have recently received considerable attention (see Köylü and Faeth [12], Farias *et al.* [13] and the references cited therein). These investigations, however, were generally limited to fundamental optical cross sections at visible wavelengths because of their specific interest in developing tools for laser diagnostics in particulate-laden media.

† Author to whom correspondence should be addressed. Tel.: 001 305 348 1864. Fax: 001 305 348 1932. E-mail: koyluu@eng.fiu.edu.

NOMENCLATURE

C	optical cross section
d_p	diameter of a soot primary particle
D_f	mass fractal dimension of soot aggregates
$\mathbf{E}$	internal electrical field of each particle within an aggregate
$e_{b\lambda}$	spectral hemispherical blackbody flux
$\mathbf{E}_{inc}$	incident electric field
f_v	soot volume fraction
i	$\sqrt{-1}$
j	index variable
j_1	first-order spherical Bessel function of the first kind
k	wave number, $2\pi/\lambda$
K	optical coefficient
k_f	fractal prefactor
l	index variable
L	optical path length
m	complex refractive index of soot
N	number of primary particles in an aggregate
R_g	radius of gyration
s	self-interaction coefficient
$\bar{\mathbf{T}}$	scattering matrix
V	particle/aggregate volume
x_p	optical size parameter of a soot primary particle, $\pi d_p/\lambda$
z	propagation direction of electrical field.

Greek symbols

ε_λ	spectral soot emissivity
ε_T	total soot emissivity
η	real part of soot refractive index
θ	scattering angle
κ	imaginary part of soot refractive index
λ	wavelength of radiation
Φ	phase function
Ω	single-scattering albedo.

Subscripts

a	absorption
d	differential scattering
e	extinction
s	total scattering.

Superscripts

a	aggregate
p	particle.

The main objective of the present study was to quantitatively analyze the effects of the soot shape on radiative transfer predictions in soot-containing flames by using a realistic simulation of the aggregation process. Various spectral properties (phase function, albedo, extinction coefficient, and emissivity) of fractal soot aggregates were computed for a broad wavelength spectrum from ultraviolet (0.2 μm) to infrared (6.2 μm). Total emissions from uniform clouds of aggregates of spherical particles were then estimated for typical volume fractions and flame temperatures. The computations for aggregates were performed based on the integral equation formulation for scattering (IEFS), which accounts for multiple scattering and interactions among small spherical particles [14, 15]. IEFS formulation was applied to simulated aggregates having a prescribed primary particle diameter, a number of primary particles in an aggregate, and a fractal dimension that are representative of soot-like morphologies typically found in flame environments [5, 16]. All radiative properties of soot aggregates computed from IEFS were normalized by the predictions based on the same formulation for primary (unaggregated) particles using the spectral refractive indices determined by Chang and Charalampopoulos [17]. This normalization allowed a quantitative comparison between the radiative properties of complex shape aggregates and those of simple spherical particles composing them and led to the possible development of simple tools for the engineering treatment of radiative modeling of combustion devices.

2. THEORETICAL METHODS

2.1. *General*

In order to apply the fundamental equation of radiative transfer to absorbing, emitting and scattering media of particulate-containing combustion systems (excluding the effects of gas radiation), it is necessary to know several spectral properties, namely the extinction coefficient ($K_{e\lambda}$), albedo (Ω_λ), and phase function (Φ_λ), which are defined in terms of optical coefficients as follows:

$$K_{e\lambda} = K_{a\lambda} + K_{s\lambda} = \frac{K_{a\lambda}}{1-\Omega_\lambda} \tag{1}$$

$$\Omega_\lambda = \frac{K_{s\lambda}}{K_{e\lambda}} \tag{2}$$

$$\Phi_\lambda(\theta) = 4\pi \frac{K_{d\lambda}(\theta)}{K_{s\lambda}}. \tag{3}$$

On the other hand, radiation heat-flux rates along a uniform column of suspended aerosols require an estimate of total emissivity, defined as:

$$\varepsilon_T = \frac{1}{\sigma T^4}\int_0^\infty \varepsilon_\lambda e_{b\lambda}\,d\lambda \quad (4)$$

where the spectral emissivity for an absorbing and scattering medium is given by

$$\varepsilon_\lambda = 1-\exp\left[-\left(\frac{K_{e\lambda}}{f_v}\right)f_v L\right]. \quad (5)$$

2.2. *Radiative predictions for aggregated spherical particles*

The integral equation formulation for scattering (IEFS) was employed in this study to compute the radiative characteristics of soot aggregates. The following description of this theoretical method is brief; additional details can be found in refs. [10, 13–15].

The IEFS method divides an aggregate into sufficiently small units so that the internal field within each particle is assumed to be uniform. By considering not only the phase differences but also the multiple scattering and self-interaction terms, the internal electrical field of each particle, $\mathbf{E}_j$, is then obtained from the following system of $3N\times 3N$ linear equations:

$$\mathbf{E}_j = \left(\frac{3}{m^2+2}\right)\mathbf{E}_{\text{inc},j} + i\left(\frac{m^2-1}{m^2+2}\right)x_p^2 j_1(x_p) \times \sum_{l=1,\neq j}^{N} \bar{\mathbf{T}}_{jl}\mathbf{E}_l + s_j\mathbf{E}_j;\quad j=1,2,\ldots,N \quad (6)$$

where $m=\eta+i\kappa$ represents the complex refractive index of each small particle, $\mathbf{E}_{\text{inc}}=\mathbf{E}_0\exp(ikz)$ represents the incident electric field propagating along the z axis with a wave number of $k=2\pi/\lambda$, $j_1(x_p)$ is the first-order spherical Bessel function of the first kind, and $\bar{\mathbf{T}}$ is the scattering matrix. Once the internal field of each spherical particle is known from equation (6), various optical cross sections that are needed in the calculation of the extinction coefficient, albedo, phase function, and emissivity [equations (1)–(5)] can be obtained for an aggregate with N uniform size particles (see, e.g., Farias *et al.* [15] and references cited therein). For example, the spectral extinction coefficient, $K_{e\lambda}$ normalized by the soot volume fraction, f_v, is expressed as follows:

$$\frac{K_{e\lambda}}{f_v} = \frac{3k}{N}\frac{j_1(x_p)}{x_p} Im\left[(m^2-1)\sum_{j=1}^{N}\mathbf{E}_{\text{inc}}^{*}\cdot\mathbf{E}_j\right]. \quad (7)$$

This formulation satisfies the optical theorem, i.e., the sum of the total scattering and absorption cross sections is exactly equal to the extinction cross section of an aggregate [18]. Unfortunately, the IEFS method is computationally intensive for treating relatively large and/or polydisperse soot aggregates. Notice that the accuracy of the solution will be somewhat influenced at very short wavelengths (0.2–0.4 μm) because the approximation of uniform electric field within each primary particle starts failing in this ultraviolet portion of the spectrum. Furthermore, the uniform-field assumption may be less accurate for aggregates of touching spheres that have large $\eta\kappa$, e.g., soot optical characteristics in the far-infrared wavelengths (see Mackowski [19, 20] and references cited therein).

To compute the radiative properties of complex aggregate structures, it was necessary to know the primary particle positions within each aggregate. It has been shown that soot aggregates follow a mass fractal-like morphology that can be represented by $N=k_f(R_g/d_p)^{D_f}$, where N is the number of primary particles in an aggregate, R_g is the radius of gyration, d_p is the primary particle diameter, and D_f is the fractal dimension [4, 5]. Aggregates were created using a practical sequential algorithm that models this statistical fractal relationship rather than the formal diffusion-limited cluster-cluster (DLCC) simulations [13, 15]. Briefly, the aggregation process was initiated by randomly attaching individual and pairs of particles to each other. The radius of gyration of the new aggregate was calculated by definition from the positions of each primary particle and checked if it satisfied the above-mentioned fractal relationship with $D_f\approx 1.8$. This procedure was continued in order to form progressively larger clusters. Thirty-two different realizations of the same aggregate size, each sampled at 16 different orientations, were averaged to obtain statistically significant IEFS predictions with less than 10% numerical uncertainties (95% confidence interval).

The computational parameters of the present investigation were chosen based on the previous experimental results within soot-containing flames. In spite of the complex appearance, various size and shape soot aggregates have been found to have a universal morphology with $D_f=1.6$–1.9 and $k_f=7$–9, almost independent of the fuel source and flame position. Additionally, it has been observed that the size of soot particles could be adequately represented by a mean diameter (generally between 20 and 50 nm) because of the relatively narrow size distribution at a particular flame location. As a result, only aggregates with $D_f\approx 1.8$, $k_f\approx 8$, and $d_p=30$ nm were considered during this study. The number of primary particles within an aggregate, N, was varied from 1–256, typical of soot in various combustion environments. It must be emphasized that our objective was to investigate only the real soot aggregates found in real flames, i.e., fractal-like aggregates formed from uniform-size small spherical particles. Thus, unrealistic shapes, such as cylinder-like and sphere-like aggregates, will not be considered here.

Soot refractive indices inferred by Chang and Charalampopoulos [17] were employed in this study because of their consistency with numerous experiments as well as because of their spectral accuracy in the ultraviolet wavelengths. Table 1 summarizes these spectral values of η and κ for soot at the lowest position in a propane-fueled premixed flame with fuel equivalence ratio of 1.8. These values reported in ref. [17] have also been supported by recent independent

Table 1. Spectral refractive indices of soot used in this work (as inferred by Chang and Charalampopoulos [17])

λ (μm)	η	κ
0.20	0.78	0.32
0.26	1.04	0.78
0.40	1.50	0.65
0.54	1.63	0.48
0.71	1.61	0.47
1.00	1.65	0.50
2.16	1.83	0.75
3.89	2.10	1.11
6.24	2.33	1.41

investigations involving diverse flame conditions (see Köylü and Faeth [21] and references cited therein).

3. RESULTS AND DISCUSSION

Spectral radiative properties of soot, namely phase function, albedo, extinction coefficient and emissivity, were computed for a wide range of wavelengths from 0.2–6.2 μm. The numerical IEFS results were normalized by the primary particle properties using the same scattering theory so that the effects of the aggregation process on the soot radiation transport can be presented. Spectral extinction and emissivity computations involved uniform clouds (optical path length, L) of monodisperse aggregates (soot volume fraction, f_v) having $f_vL = 10^{-8}$–10^{-6} at typical flame temperatures of $T = 1500$–2000 K. Note that the consideration of non-uniform path lengths will not affect our findings. A brief discussion of the phase function and albedo at various wavelengths were also included for completeness with respect to all the fundamental properties appearing in the radiative transfer equation.

3.1. *Phase function and albedo*

Figure 1 illustrates the ratio of the phase function of soot aggregates to that of primary particles at two wavelengths, 0.4 and 1.0 μm. It is evident that this ratio depends strongly on the number of primary particles in an aggregate, N, and the scattering angle, θ, especially in the ultraviolet (UV) and visible (VIS) portions of the wavelength spectrum. For example, the phase function for the case of $N = 256$ is enhanced by almost an order of magnitude in the forward direction for $\lambda = 0.4$ μm as a result of the aggregation process. However, the phase function ratio, Φ^a/Φ^p, flattens out with increasing wavelength, eventually becoming unity in the infrared (IR) region.

The ratio of albedo of soot aggregates to that of primary particles as a function of wavelength is shown in Fig. 2 for various aggregation levels. The albedo certainly increases with increasing N, reaching one to two orders of magnitude enhancement for $N = 256$ over that of unaggregated primary particles. Moreover, Ω^a/Ω^p also increases with λ before saturating in

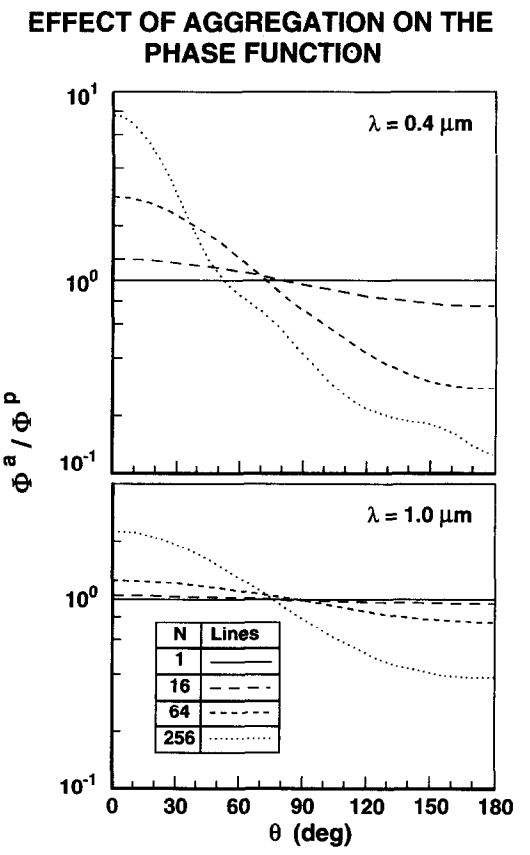

Fig. 1. The effect of aggregation of small spherical soot particles on the phase function at two wavelengths of 0.4 and 1.0 μm.

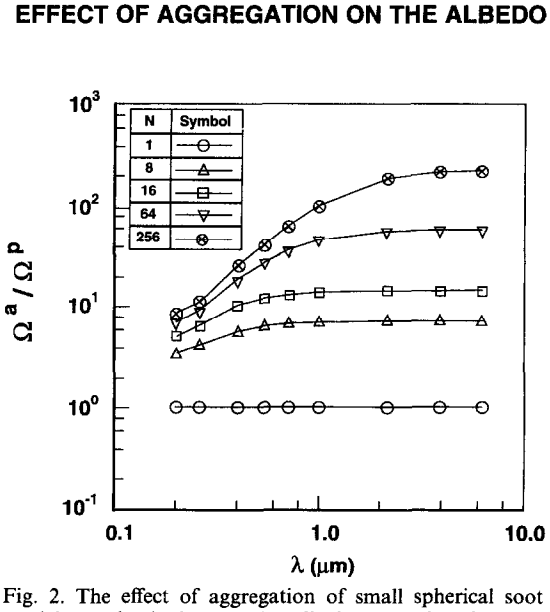

Fig. 2. The effect of aggregation of small spherical soot particles on the single-scattering albedo at wavelengths ranging from 0.2–6.2 μm.

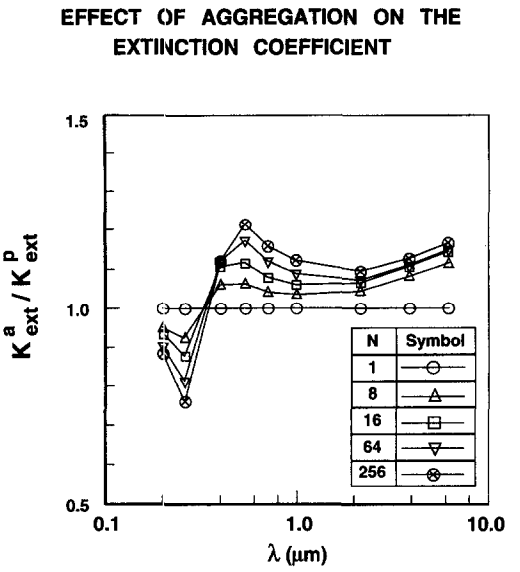

Fig. 3. The effect of aggregation of small spherical soot particles on the spectral extinction coefficient.

the IR portion of the wavelength spectrum, in which the effect of scattering is negligible. It should be noticed that, in the IR region, the albedo of aggregates relative to that of primary particles approaches the value N, independent of the refractive index, primary particle diameter, and wavelength. In other words, because $K_c \sim V$ and $K_s \sim V^2$ for particles in the Rayleigh limit, it is expected that $\Omega^a/\Omega^p \sim V^a/V^p \sim N$ in the IR. In general, these results related to the phase function and albedo have important consequences in the interpretation of *in situ* optical measurements.

3.2. *Spectral extinction coefficient*

The effect of aggregation of small soot particles on the spectral extinction coefficient is presented in Fig. 3 for various N in the range 1–256. The ratio, K_e^a/K_e^p, corresponds to the aggregate extinction normalized by that calculated for N independent (non-interacting) spherical particles. As can be seen from Fig. 3, the ratio of the extinction coefficient of aggregates to that of primary particles noticeably deviates more from unity as the coagulation of soot particles leads to larger clusters. On the other hand, the spectral variation of the relative aggregate extinction coefficient has an interesting and somewhat unexpected behavior: K_e^a/K_e^p is less than one for $\lambda < 0.3$ μm, after which it increases to reach a maximum value of 25% at $\lambda = 0.54$ μm for $N = 256$. Then, it shows a declining trend from VIS to near-IR before increasing again in the IR region. The complicated behavior of the spectral extinction coefficient can be understood by considering the effect of the soot refractive index in parallel to the aggregate growth process.

Similar to the trends in the VIS, the extinction coefficient of aggregates was expected to keep increasing in the UV because of the continuous effect of aggregate scattering enhancement with decreasing wavelength. However, after $\lambda = 0.54$ μm, K_e^a/K_e^p decreases, reaching a minimum at 0.26 μm, apparently related to a resonance effect of soot refractive indices at this wavelength range [17, 21, 22]. This interesting behavior of extinction in the UV is a result of the fact that the absorption cross section of an aggregate is less than that of separate (non-touching) primary particles with the same number, that is $C_a^a < NC_a^p$. Therefore, reduced absorption balances enhanced scattering, attenuating the extinction coefficient of aggregates relative to that of individual particles composing them. These observations have significant implications with respect to the extinction measurements at short wavelengths because they suggest that the aggregation process causes less than 25% deviation in the extinction coefficient, rather than having a notorious effect for short wavelengths.

Another striking feature of the extinction coefficient can be found in the IR region, in which K_e^a/K_e^p starts increasing. This is also somewhat against the anticipation that the extinction coefficient of aggregates should be identical to that of primary particles as the wavelength increases. The underlying logic behind this expectation is that aggregate scattering becomes negligible in the IR and absorption is not affected by aggregation. Nevertheless, as observed in the UV, the spectral variation of the soot refractive indices also plays an important role in the IR. There are contrasting effects of wavelength and soot refractive indices on K_e^a/K_e^p at large wavelengths: larger λ reducing the effect of scattering due to the decrease in x_p, while larger m leads to more deviations in the absorption coefficient. In other words, as the wavelength starts increasing in the near-IR, extinction coefficient is to decrease due to a decline in x_p, but at the same time there will be an increase in K_e due to an increase in both η and κ. These opposite effects appear to balance in the near-IR, resulting in a minimum at about $\lambda = 2$ μm in Fig. 3. It is anticipated that the aggregation of primary particles into fractal clusters will lead to a further enhancement in the extinction coefficient for larger wavelengths because the continuous increase in the soot refractive indices in the IR will substantially influence the electric field inside the particles [19, 20].

3.3. *Spectral emissivity*

Figure 4 illustrates the ratio of spectral emissivity of soot aggregates to that of primary particles for various uniform clouds of soot with $f_vL = 10^{-8}$–10^{-6}. Although only emissivities for small ($N = 16$) and large ($N = 256$) aggregate sizes were shown, the results for other sizes in between were similar. Because of the relationship between ε_λ and K_e given by equation (5), the spectral behavior of soot emissivity follows closely that of the extinction coefficient (see Fig. 3). For a specific aggregate size, the ratios of spectral emissivities of soot aggregates to those of unaggregated primary particles generally increase from UV to VIS and decrease from VIS to near-IR before a

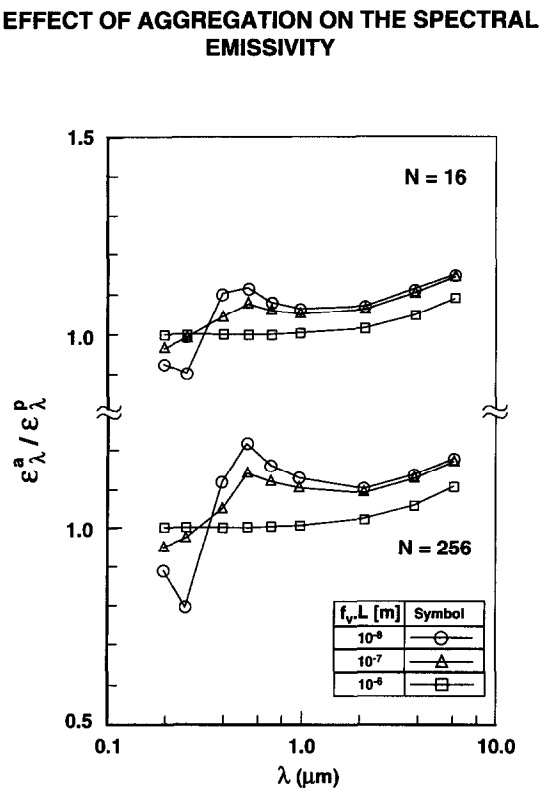

Fig. 4. The ratio of spectral emissivity of aggregates to that of primary particles for various uniform clouds of suspended soot with $f_vL = 10^{-8}$–10^{-6}.

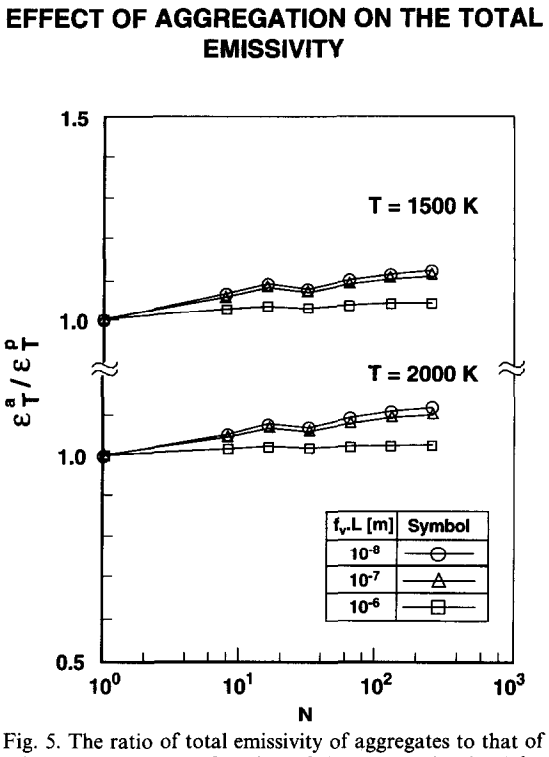

Fig. 5. The ratio of total emissivity of aggregates to that of primary particles as a function of the aggregation level for isothermal clouds of soot with typical volume fractions and flame temperatures.

continuous increase in the IR. The reasons for this relatively complex behavior are related to the total scattering and absorption properties of aggregates that are also functions of soot refractive indices, as discussed in the previous section. $\varepsilon^a_\lambda/\varepsilon^p_\lambda$ deviates more from unity as the clusters grow as a result of the aggregation process. Additionally, the relative spectral emissivity of a uniform path length of soot aggregates approaches unity as the product of f_v and L becomes large. This is consistent with equation (5), which states that $\varepsilon_\lambda \to 1$ in the case of optically thick limit, independent of the soot particle shape. In all the cases considered in this investigation, the effect of aggregation on the spectral emissivity of soot never exceeded 25% for typical flame conditions.

3.4. *Total emissivity*

Total emissivities of isothermal clouds of soot aggregates relative to that of unaggregated primary particles are shown in Fig. 5 for various degrees of aggregation and typical flame temperatures of $T = 1500$ and 2000 K. It is clear that the results are relatively insensitive to the flame temperature. Moreover, the ratio $\varepsilon^a_T/\varepsilon^T_e$ is always in the range of 1.00–1.13 for the parameters considered in this study. In other words, the difference between the total emissivities of soot aggregates and individual particles composing them is usually less than 13%, implying that radiation properties of soot aggregates can be treated by considering only the unaggregated primary particles. At this point, it is timely to mention the sensitivity of the results to the uncertainties in η and κ because of the long-standing controversy surrounding the soot refractive index in the literature. For example, if the data from ref. [6] rather than ref. [17] were used, the spectral emissivity would differ somewhat (5–50%), especially in the UV to VIS wavelengths. On the other hand, the total emissivity of an aggregate cloud relative to that of a particle cloud would not exceed 16%. In view of these uncertainties in the soot refractive indices, the consideration of soot aggregation appears to be unnecessary for rational emissivity calculations in luminous flames. This suggests that the shape effects on emission predictions in soot-laden flames can be neglected, i.e., complex aggregates of various shape and size can be approximated as independent (non-interacting) small spherical particles for predictions of spectral and total emissivity in flames. These findings have significant implications in many engineering applications because they vastly simplify the treatment of radiation modeling of combustion devices.

4. SUMMARY AND CONCLUSIONS

The effects of soot shape on radiative transfer predictions in soot-containing flames were quantitatively

analyzed by using a realistic simulation of the aggregation process. Various spectral properties (phase function, albedo, extinction coefficient, and emissivity) of fractal soot aggregates were computed using the integral equation formulation for scattering (IEFS) for a broad wavelength spectrum from ultraviolet (0.2 μm) to infrared (6.2 μm). Total emissions from uniform clouds of aggregates of spherical particles were then estimated for typical volume fractions and flame temperatures. Using typical soot refractive indices, all spectral and total radiative transfer properties computed using IEFS were normalized by the predictions based on the same formulation for primary (unaggregated) particles. Main conclusions of the present study can be summarized as follows:

(1) The spectral variation of the extinction coefficient of aggregates relative to that of primary particles has a somewhat unexpected and complex behavior in the ultraviolet and infrared wavelength regions due to the opposite effects of aggregation and soot refractive indices.
(2) The effects of soot morphology on spectral and total emissivities are found to be relatively small (less than 25 and 13%, respectively), for typical soot volume fractions and flame temperatures.
(3) The results clearly suggest that the shape effects on emission predictions in soot-laden flames can be neglected, vastly simplifying the engineering treatment of radiation modeling of combustion devices.

Acknowledgements—The authors would like to thank Prof. Daniel E. Rosner of Yale University for his valuable suggestions. One of the authors (Ü.Ö.K.) was partially supported by funds provided by Florida International University.

REFERENCES

1. Tien, C. L. and Lee, S. C., Flame radiation. *Prog. Energy Combust. Sci.*, 1982, **8,** 41–59.
2. Viskanta, R. and Mengüç, M. P., Radiation heat transfer in combustion systems. *Prog. Energy Combust. Sci*, 1987, **13,** 97–160.
3. Siegel, R. and Howell, J. R., *Thermal Radiation Heat Transfer*. Hemisphere, New York, 1992, pp. 658–669.
4. Megaridis, C. M. and Dobbins, R. A., Morphological description of flame-generated materials. *Combust. Sci. Tech.*, 1990, **77,** 95–109.
5. Köylü, Ü. Ö. and Faeth, G. M., Structure of overfire soot in buoyant turbulent diffusion flames at long residence times. *Combust. Flame*, 1992, **89,** 140–156.
6. Lee, S. C. and Tien, C. L., Effect of soot shape on soot radiation. *J. Quant. Spectrosc. Radiat. Transfer*, 1983, **29,** 259–265.
7. Mackowski, D. W., Altenkirsch, R. A., Mengüç, M. P. and Saito, K., Radiative properties of chain-agglomerated soot formed in hydrocarbon diffusion flames. *22nd International Symposium on Combustion*. The Combustion Institute, Pittsburgh, 1988, pp. 1263–1269.
8. Charalampopoulos, T. T. and Hahn, D. W., Extinction efficiencies of elongated soot particles. *J. Quant. Spectrosc. Radiat. Transfer*, 1989, **42,** 219–228.
9. Charalampopoulos, T. T. and Chang, H., Effects of soot agglomeration on radiative transfer. *J. Quant. Spectrosc. Radiat. Transfer*, 1991, **46,** 125–134.
10. Ku, J. C. and Shim, K.-H., Optical diagnostics and radiative properties of simulated soot agglomerates. *Journal of Heat Transfer*, 1992, **113,** 953–958.
11. Kumar, S. and Tien, C. L., Effective diameter of agglomerates for radiative extinction and scattering. *Combust. Sci. Tech.*, 1989, **66,** 199–216.
12. Köylü, Ü. Ö. and Faeth, G. M., Radiative properties of flame-generated soot. *Journal of Heat Transfer*, 1993, **115,** 409–417.
13. Farias, T. L., Carvalho, M. G., Köylü, Ü. Ö. and Faeth, G. M., Computational evaluation of approximate Rayleigh–Debye–Gans/fractal aggregate theory for the absorption and scattering properties of soot. *Journal of Heat Transfer*, 1995, **117,** 152–159.
14. Lou, W. and Charalampopoulos, T. T., On the electromagnetic scattering and absorption of agglomerated small spherical particles. *J. Physics D: Appl. Phys.*, 1994, **27,** 2258–2270.
15. Farias, T. L., Carvalho, M. G. and Köylü, Ü. Ö., The range of validity of the Rayleigh–Debye–Gans theory for optics of fractal aggregates. *Appl. Opt.*, 1996, **35,** 6560–6567.
16. Köylü, Ü. Ö., Xing, Y. and Rosner, D. E., Fractal morphology analysis of combustion-generated aggregates using angular scattering and electron microscope images. *Langmuir*, 1995, **11,** 4848–4854.
17. Chang, H. and Charalampopoulos, T. T., Determination of the wavelength dependence of refractive indices of flame soot. *Proceedings of the Royal Society of London A*, 1990, **430,** 577–591.
18. Bohren, C. F. and Huffman, D. R., *Absorption and Scattering of Light by Small Particles*. Wiley, New York, 1983, pp. 69–81.
19. Mackowski, D. W., Calculation of total cross sections of multiple-sphere clusters. *J. Opt. Soc. Amer. A*, 1994, **11,** 2851–2860.
20. Mackowski, D. W., Electrostatics analysis of radiative absorption by sphere clusters in the Rayleigh limit: application to soot particles. *Appl. Opt.*, 1995, **34,** 3535–3545.
21. Köylü, Ü. Ö. and Faeth, G. M., Spectral extinction coefficients of soot aggregates from turbulent diffusion flames. *Journal of Heat Transfer*, 1996, **118,** 415–421.
22. Menna, P. and D'Alessio, A., Light scattering and extinction coefficients for soot forming flames in the wavelength range from 200 nm to 600 nm. *19th International Symposium on Combustion*. The Combustion Institute, Pittsburgh, 1982, pp. 1421–1428.